Biophysical Chemistry 151 (2010) 29–33

Contents lists available at ScienceDirect

Biophysical Chemistry

journal homepage: http://www.elsevier.com/locate/biophyschem

Towards modeling molecular cooperativity on the cellular scale

F.N. Braun

University of Tromsø, N-9037 Tromsø, Norway

ARTICLE INFO

Article history:
Received 25 March 2010
Received in revised form 28 April 2010
Accepted 29 April 2010
Available online 6 May 2010

Keywords:
Energy landscape
Osmoregulation

ABSTRACT

Formulated originally to describe the subtle blend of kinetics and thermodynamics that drives protein folding and ligand binding, the molecular cooperativity concept extrapolates readily to the cellular scale. Here it constitutes a thermally driven mode of cytological organization which can be provisionally explored within the equation of state (EOS) framework of classical statistical mechanics. We give a unified EOS account of the 'proto-cooperative' phenomena of phase separation and gelation in cytoplasm, emphasizing osmoregulatory control mechanism. In an extension to this framework, we show that a significant thermodynamic partitioning of ribosomes could occur spontaneously in conjunction with phase separation. This would be tantamount to a translation–transcription decoupling, with relevance to cellular evolution.

1. Introduction

Meaningful simulation of an entire biological cell has long been one of the loftier goals of computational Newtonian dynamics. In certain respects it is already achievable on today's laptops; for example in simulations of the constricting effect of crowding on diffusional timescales governing the approach of enzymes to their targets [1]. But 'cooperative' effects occurring on the whole-cell scale, such as the formation of subcellular compartments, arguably present a more considerable challenge, raising the bar somewhat.

As in the case of protein folding, the natural theoretical starting point for understanding this cytological dimension to cooperativity is the equilibrium thermodynamics concept of a phase transition: The early coil–globule phase change description of folding remains a phenomenologically correct first base for tertiary structural prediction [2]. So it is reasonable to suppose that phase behavioral idealization is also a valid initial template for cooperativity acting on larger lengthscales.

If the degree of idealization is very high, then explicit molecular dynamics becomes overkill. The Newtonian equations of motion can instead be absorbed into an analytically tractable 'equation of state' (EOS) derived via classical statistical mechanics. A successful example is Odijk's treatment of compaction of the bacterial nucleoid [3]. To describe compaction as a whole-cell cooperative phenomenon driven by volume exclusion, Odijk relied on an extremely simple hard sphere EOS to represent the cell's entire protein complement, deriving a theoretical picture remarkably consistent with subsequent experiments [4].

A second motivation for EOS idealization is to link Newtonian dynamics to an energy landscape description [5], since the landscape view affords probably the best intuitive feel for what sets biological cooperativity apart from ordinary matter: Whereas for ordinary liquids a temperature quench into the low-lying slopes of the landscape ends in the arrested structural randomness of a glass transition, in a cooperative system these slopes are negotiated in a more directed fashion [6].

Thus while in the not-too-distant future it should be possible to model whole cells via simulations accounting fairly comprehensively for the huge array of molecular species and interactions involved, there certainly exists an interim role for the pared-down EOS approach. With these remarks for motivation, our purpose in the following is to apply EOS description to 'proto'-cooperativity interpretations of (i) subcellular compartmentation; and (ii) translation–transcription decoupling.

The point (i) that phase behavior provides a coarse mechanism for subcellular compartmentation is already qualitatively established [7,8], and the first part of our discussion will serve just to put it on an EOS footing, adequately primed for the more novel direction (ii). We technically review the two distinct phase behavioral phenomena implicated in subcellular compartmentation: Liquid–liquid phase separation, which will tend to drive the formation of bubbles with cytosol-like macromolecular concentrations; versus gelation, which we associate with denser compartments with inclusion body consistency [9–13]. To describe gelation, it is natural to use the energy landscape picture, although at this stage we do not attempt to specifically introduce a cooperative element. In Section 4 we address the modulation of phase behavior by compatible osmolytes. This is of interest because by implication compatible osmolytes provide a mechanism for regulatory control of cooperativity.

The last section adapts the EOS framework to accommodate ribosome partitioning under a phase separation. When such partitioning is strong, it constitutes a transition–transcription decoupling,

E-mail address: f.n.braun@gmail.com.

0301-4622/$ – see front matter © 2010 Elsevier B.V. All rights reserved.
doi:10.1016/j.bpc.2010.04.008

our item (ii) above. So here there exists a tentative link to the nuclear compartmentation event which marks the cell–evolutionary transition from prokaryote to eukaryote.

2. Cytoplasmic phase separation

We base everything on an orthodox 'colloidal' mode of EOS description which is known to successfully capture the main phase behavioral features exhibited by in vitro protein solutions [14,15]. The term 'colloidal' applies loosely to any solvated suspension of microscopic particles, tending to attract one another (Latin inf. *colligere* = clump together), though not strongly with respect to the thermal energy kT. It is worthwhile to stress that as a paradigm for treating protein–protein interaction, this is somewhat removed from structural biology. The specific aspect of biochemical molecular recognition is not at all of the essence in the colloidal view. The focus is instead on the sort of non-specific interactions which occur during random collisions, comprising sphere-like volume exclusion (i.e. crowding [16]), salt-attenuated electrostatics, dispersion forces and the hydrophobic effect.

Sear has pointed out that these pose a promiscuous distraction to specific binding partners, a sort of noisy hubbub over which they must shout to be heard [17]. However, the label 'non-functional' adopted on this basis by Zhang et al. [18], in performing an analysis similar to Sear's, is a misnomer. Notably in this respect, Hlevnjak et al. [19] have recently looked for and found evidence that known groups of co-localized proteins tend to share various coarse-grained physicochemical features in common, substantiating a functional role for non-specific interactions in connection with subcellular compartmentation.

From the EOS modeling perspective, there is a major *ansatz* to be made by noting that the colloidal components we have listed are all nearest-neighbor interactions in the statistical mechanical sense, and so may be feasibly lumped together in a single effective square well, or some similarly short-ranged model potential such as the Baxter or Yukawa [15,20,21]. Quite sophisticated EOS methods exist for such potentials [22], but it is sufficient for our purpose to go with the elementary Van der Waals form

$$\Pi = \rho kT / (1-\varphi) - 2\pi\varepsilon a d^2 \rho^2. \tag{1}$$

Irrespective of their relative sophistication, all EOSs have this same essential anatomy in common: Thermodynamics on the l.h.s., in this case osmotic pressure Π, is defined analytically with respect to microscopic interactions and structure on the r.h.s. The set of microscopic parameters in this particular instance comprises ρ for protein concentration, d for the protein lengthscale (i.e., an effective diameter), and $\varphi = \pi\rho d^3/6$ for the protein-occupied volume fraction. Well depth and range are denoted respectively by ε and a, but it is convenient in practice to absorb these into a dimensionless 'attraction' $\alpha = 3(a/d)\varepsilon/kT$, so that $\Pi/\rho kT = 1/(1-\varphi) - 4\alpha\varphi$. Cellular protein volume fractions lie typically around $\varphi = 20$–30%, while for a realistic selection of parameter values $d = 6$ nm, $a = 1$ nm, and $\varepsilon = 2kT$ we expect $\alpha \approx 1$.

Phase separation is read off the EOS as the locus of diverging compressibility $\partial\rho/\partial\Pi \to \infty$, the 'spinodal'. The phase separating domain of (φ, α) extends off the spinodal's extremum, the venerable Van der Waals 'critical point' $\varphi_c = 1/3$; $\alpha_c = 27/32$. Insofar as this falls within what we expect to be the physiological region of (φ, α), it verifies that phase behavioral effects are well within striking distance of a real cytoplasm.

3. Cytoplasmic gelation

There exist a number of rival theories of gelation. The landscape one takes precedence in the present context primarily because of the traditional association of landscapes with biological cooperativity we already remarked on. However, it also has the virtue that it derives easily from first principles [5,21]. Briefly, the high terrain of the landscape represents states in which there are very few attractive bonds between the cell's protein components, hence the interaction enthalpy per particle is negligible, $e \approx 0$. The low terrain on the other hand corresponds to states in which the proteins are lumped in clusters [23] so that e becomes significant. With decreasing thermal energy kT relative to landscape topology, these low-lying states become increasingly difficult to escape from, until the system finally gels. Mathematically this onset is distilled by the device of an ideal glass, a single nondegenerate state at the very bottom of the landscape, characterized by $e = e_{ig}$ and zero per-particle entropy $s = 0$. When the condition $(\partial f/\partial e)_{e_{ig}} = 0$ is met, where f is the Helmholtz free energy, the ideal glass becomes thermodynamically stable.

The condition is solved by writing $f = e - Ts(e)$ and invoking a quadratic interpolation $s(e)/s^* = 1 - (e/e_{ig})^2$, to yield

$$T_{gel} = e_{ig} / \left(2s^*\right), \tag{2}$$

where s^* is similar to the usual Van der Waals translational entropy $s/k = \ln(1-\varphi) - \ln\varphi + \text{const}$, but subject to the constraint there are no bonds in the system. We can neatly implement this constraint just by renormalizing effective particle diameter from d to $d + a$, where a is the bonding range,

$$s^*/k \approx ln\frac{1-\gamma\varphi}{\gamma\varphi} + \text{const}, \tag{3}$$

where $\gamma = 1 + 3a/d$. The constant is fixed by requiring $T_{ig} \to \infty$ in the random close packing limit $\varphi = 0.64$. Substituting back into Eq. (2) the result for the gelation volume fraction is then

$$\varphi_{gel} = \left[\gamma + (1/0.64 - \gamma) exp\left(e_{ig}/2kT\right)\right]^{-1}. \tag{4}$$

If we write $e_{ig} = -n_{ig}\varepsilon/2$, where $n_{ig} \simeq 4$ is a reasonable guess for the average number of nearest-neighbor bonds per protein in the gel phase, then in the (φ, α) projection we have roughly

$$\alpha_{gel} \approx \frac{1}{2} ln\left(\frac{2}{3\varphi} - 1\right) + \frac{3}{2}. \tag{5}$$

This result is not just so much pie-in-the-sky! An applied biotechnological arena where it is conceivably of practical use is in predicting the odds on successful recombinant protein expression. A web-based bioinformatic tool devised along such lines can be accessed at https://sites.google.com/site/dewcheckcell/.

4. Compatible osmolytes

Should phase behavior slip out of regulatory control, then clearly it can easily end up being highly detrimental to a cell's wellbeing, as happens in the well documented sickle cell and Alzheimer pathologies. Control is arguably enforced at least in part by evolutionary negative selection, acting on expression levels in particular [24,25]. On the other hand, for the cell to actively maneuver around a phase diagram in the dynamic manner we anticipate for cooperativity effects, there must presumably also exist more immediate physiological mechanisms, to which the cell has recourse 'in real-time'. The most obvious candidate for this is just the usual means by which a cell safeguards its osmotic wellbeing, regulation of its internal osmolyte concentration.

In addition to ordinary salts, the cell scavenges the environment for small organic molecules such as glycine betaine [26] which are of premium 'compatible' osmoregulatory character in that they do not

interfere with biological macromolecules except by volume exclusion. One of the several functions of compatible osmolytes (COs) appears to be to suppress or exercise control over phase behavior. In particular, Bogaart et al. [27] report discrete pools of subcellular diffusional confinement in bacterial cells, which we interpret here as phase-separated bubbles. The bubbles are reversibly induced by osmotic stress, but do not appear at all if COs are in the growth medium.

The effect can be understood theoretically by supplementing Eq. (1) with an additional entropic contribution [28]

$$\Pi_{co} = \rho_{co} kT / (1-\varphi) \tag{6}$$

where ρ_{co} is CO concentration. Reinspecting the spinodal line $\partial\Pi/\partial\rho \to 0$, as plotted in Fig. 1, we find that fairly modest CO uptake $\rho_{co} = 20$ mM is sufficient to move the critical point to $\alpha_c \approx 2$, away from the physiological window around $\alpha = 1$.

That CO uptake likewise alleviates gelation is empirically familiar in recombinant protein production [29]. This gelation-suppressing effect we can again attribute to CO entropy: As they become trapped in the gel matrix, their entropy is lost; hence their presence imposes an unfavorable extra energetic cost on gelation. Fig. 1 incorporates the effect by supplementing Eq. (3) with an entropic contribution derived from Eq. (6) via the standard thermodynamic relation $S/k = \partial_T \int \Pi dV$,

$$s^*_{co}/k = \frac{\rho_{co}}{\rho}\left(ln\frac{1-\varphi}{\rho_{co}} + const.\right) \tag{7}$$

again fixing the constant to ensure that α_{gel} goes to zero at $\varphi = 0.64$.

How does the cell know when regulatory action such as CO circulation is appropriate? Some form of system biological monitoring must arguably be present in order for the cell to recognize proximity to the key features of Fig. 1. There exists as yet no experimental inkling, so we consider here the purely theoretical possibility of a biochemical signaling network wired to the classical statistical mechanical signatures of impending phase behavior. (Interestingly, in an analogous spirit, it has been proposed that the statistical mechanical concept of 'critical slowing down' could provide early warning of geophysical bifurcations in the Earth system, referred to as tipping points [30].)

Recall that the approach to the spinodal line bounding phase separation corresponds by definition to a continuous divergence in osmotic compressibility. Thus, thermal fluctuations $\delta\rho$ in local protein concentration grow accordingly, the mean-square $\langle\delta\rho^2\rangle$ providing a scalar measure of how close the system is to phase separating. Proximity to the gel line, on the other hand, is straightforwardly manifested by a pretransitional decline in diffusional mobility [21].

Fig. 2 sketches in electronics shorthand an osmosensory system capable in principle of converting these respective signatures into osmoprotective stimuli. Note that we are considering here only the simplest regulatory scenario in which the cell wishes to resist phase behavior, rather than seeking to control it in some more subtle fashion.

The comparators of the sketch can be biochemically rendered by the common system biological motif of an enzymatic futile cycle [31]. Futile cycles are also able to act as signal amplifiers, with the novel property that the steady-state amplification factor G is sensitive to the degree of noise σ on the input [32]. Fig. 2 incorporates such an amplifier in series with a low-pass filter (LPF). Concentration fluctuations $\delta\rho$ fed to the amplifier are converted to a graded comparator input, and the comparator flags when some threshold $\langle\delta\rho^2\rangle$ is reached. The remaining logic operations can be achieved e.g. by various combinations of biochemically rendered nand gates [33].

5. Ribosomes

The minimal Van der Waals EOS we have invoked thus far neglects the spread of macromolecular weights which exists in a real cytoplasm; we are approximating the true 'polydisperse' distribution of effective diameters $f(d)$ by a 'monodisperse' system of particles having the same d.

Monodisperse approximation is not bad in certain respects. For instance, consider a polydisperse correction to Eq. (1) in which d^2 is replaced with the second moment $\langle d^2\rangle$ of $f(d)$, so that $\Pi/\rho kT = 1/(1-\varphi) - 4\alpha'\varphi$ where $\alpha'/\alpha = \langle d^2\rangle/d^2$. If we assume it is okay to neglect mixing entropy (more detailed analysis seems to green-light this [24]), then it follows immediately that the original critical point moves to $\alpha_c + \Delta\alpha_c = \alpha_c d^2/\langle d^2\rangle$. Substituting $\delta^2 = (\langle d^2\rangle - d^2)/d^2$ to quantify the degree of polydispersity, we have equivalently $\Delta\alpha_c/\alpha_c = -\delta^2/(1+\delta^2)$. Proteomic analysis of lysed bacterial cells reveals typically $\delta \approx 10\%$ [34], so the correction amounts to a negligible $\Delta\alpha_c/\alpha_c \approx 1\%$.

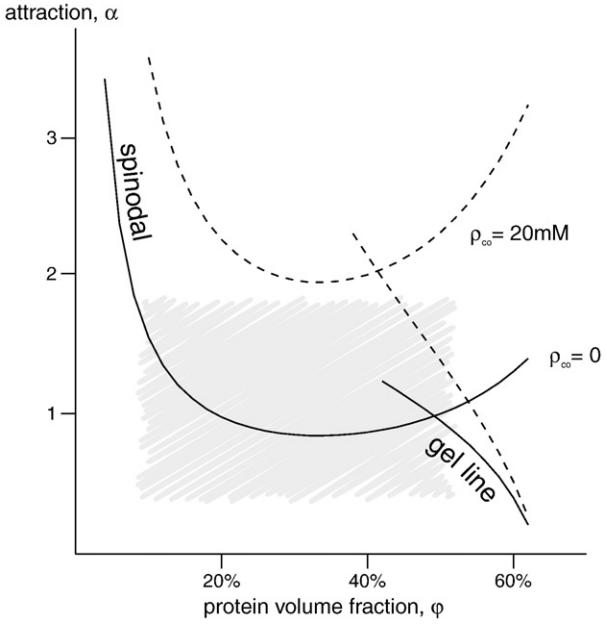

Fig. 1. Effect of CO uptake according to the Van der Waals EOS framework. Phase separation and gelation occur respectively above the spinodal and gel line. Only a subdomain of the phase space is expected to be physiologically accessible, as schematically depicted by the shaded window.

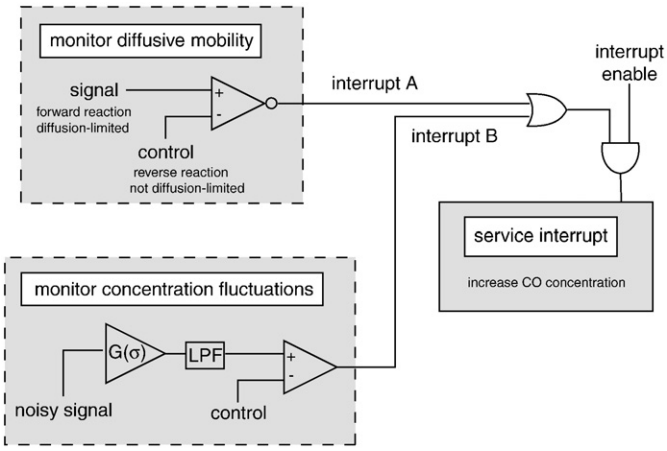

Fig. 2. Speculative system-biological scheme for osmosensing and resisting the onset of colloidal phase behavior. Interrupt A flags close proximity to the gel line, while interrupt B flags proximity to the spinodal line.

However, this is very much a protein-centric approach, and as such it misses phenomenological avenues to do with the significant colloidal presence of ribosomes (roughly 10% of the volume fraction in a bacterial cell [35]). As colloidal entities, ribosomes distinguish themselves primarily by their large relative size, about twice the diameter of a typical protein, $d_r \approx 2d_p$ [36]. So it is appropriate to incorporate them explicitly as a specific class of colloidal entity separate from proteins.

Consider to this effect a bidisperse proteome–ribosome model (BPR) of cytoplasm defined by the virial equation of state

$$\Pi / kT = \rho_p + \rho_r + \rho \mathbf{B} \rho^T, \tag{8}$$

where $\rho = (\rho_p, \rho_r)$ denotes protein (p) and ribosome (r) concentrations. Sear and Cuesta [37] have previously proposed a general virial formulation to describe cytoplasm, of which this can be considered a simple case. The interaction matrix **B** is worked through in Table 1.

We now apply this description to address what happens to the ribosomes when the cell undergoes phase separation. Do they partition preferentially into the protein-poor or protein-rich phase? Either way, such partitioning constitutes a spontaneous localization of the protein translational apparatus. This has relevance to the debate over the origin of the eukaryote nucleus, much of which revolves around the problem of establishing mechanism and rationale for the associated decoupling of translation from transcription [38,39].

Phase separation occurs in the BPR model when the lowest eigenvalue of $\mathbf{P} + 2\mathbf{B}$ goes to zero, where **P** is the 2d diagonal matrix with elements $1/\rho_p$ and $1/\rho_r$ [37]. Information concerning ribosome partitioning is contained in the corresponding eigenvector, which defines the growth mode $\delta\rho = (\delta\rho_p, \delta\rho_r)$ of the initial concentration inhomogeneity from which phase separation matures [40]. We find

$$\delta\rho_r / \delta\rho_p = \frac{-B_{rp}}{B_{rr} + B_{\mathrm{ref}} / \varphi_r} \tag{9}$$

where $\varphi_r = (\pi/6)\rho_r d_r^3$ is the ribosome volume fraction.

If this ratio is very small then ribosome partitioning is negligible. Otherwise, its sign determines whether ribosomes partition preferentially into the protein-rich or into the protein-poor phase. According to Table 1 $\delta\rho_r/\delta\rho_p \propto (\alpha - 3/2)$, and so we infer the various nuclear envelope scenarios of Fig. 3. The transcriptional apparatus of the cell (mainly RNA polymerase) can be assumed to be localized inside the envelope by the usual DNA binding equilibrium [4]. Hence in the two cases shown where ribosomes partition outside, transcription and translation have spatially decoupled. The $\alpha \simeq 3/2$ scenario on the other hand corresponds to a blindspot in ribosome–proteome interaction $B_{rp} \simeq 0$. Insofar as ribosomes do not 'see' the proteome in this sense, neither do they see it phase separate; there is no partitioning and they continue to distribute evenly across the cell. This is reminiscent of electron micrographs showing ribosome-like particles indiscriminately distributed both inside and outside an unusual membrane-bound nuclear envelope (the 'pirellulosome') found in the Planctomycetes phylum of bacteria [13].

Table 1
Definition of 2nd virial matrix components for the BPR model of cytoplasm, Eq. (8). Proteins (p) and ribosomes (r) are treated as square well particles sharing the same square well parameters ε a, but with different hard core diameters, d_p and $d_r = 2d_p$ respectively. For compactness we scale by $B_{\mathrm{ref}} = 2\pi d_p^3/3$.

	Hard core	Well	Total B_{ij}/B_{ref}
$ij = pp$	$2\pi d_p^3/3$	$-2\pi a d_p^2 \epsilon / kT$	$1-\alpha$
rp	$\pi(d_r + d_p)^3/12$	$-(\pi/2)a(d_r + d_p)^2 \epsilon / kT$	$\frac{9}{4}\left(\frac{3}{2} - \alpha\right)$
rr	$2\pi d_r^3/3$	$-2\pi a d_r^2 \epsilon / kT$	$8 - 4\alpha$

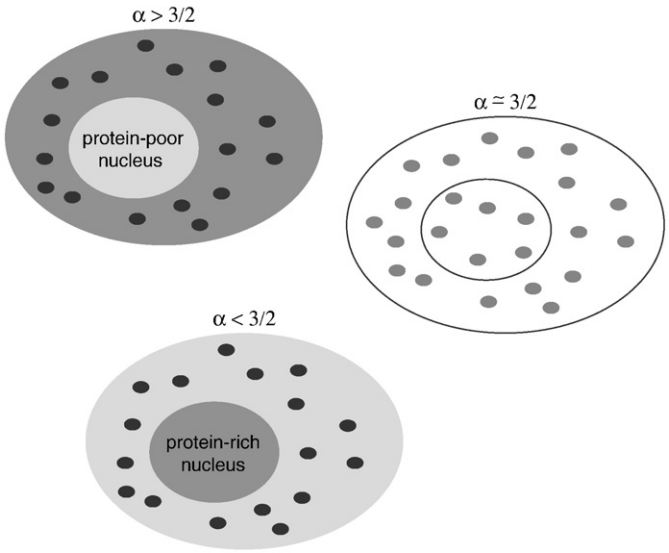

Fig. 3. In the comparatively featureless cell plan of prokaryotes, a phase-separated bubble could encapsulate the cell's DNA and transcriptional apparatus, thus forming a primitive nucleus. Spontaneous thermodynamic partitioning of ribosomes (small disks of the figure) outside the nucleus is reminiscent of eukaryotes. Negligible ribosome partitioning ($\alpha \simeq 3/2$) is reminiscent of the atypical cytology seen in the Planctomycetes phylum [13].

References

[1] F.N. Braun, W.P. Krekelberg, T.M. Truskett, Volatile diffusional character of cytoplasm, J. Phys. Chem., B 110 (2006) 25606.
[2] K.A. Dill, Theory for the folding and stability of globular proteins, Biochemistry 24 (1985) 1501–1509.
[3] T. Odijk, Osmotic compaction of supercoiled DNA into a bacterial nucleoid, Biophys. Chemist. 73 (1998) 23–29.
[4] S.B. Zimmerman, Cooperative transitions of isolated E. coli nucleoids: implications for the nucleoid as a cellular phase, J. Struct. Biol. 153 (2006) 160–175.
[5] P.G. Debenedetti, F.H. Stillinger, T.M. Truskett, C.J. Roberts, The equation of state of an energy landscape, J. Phys. Chem., B 103 (1999) 7390.
[6] K.A. Dill, H.S. Chan, From Levinthal to pathways to funnels, Nat. Struct. Biol. 4 (1997) 10.
[7] H. Walter, D.E. Brooks, Phase separation in cytoplasm, due to macromolecular crowding, is the basis for microcompartmentation, FEBS Lett. 361 (1995) 135–139.
[8] M. Long, C. Jones, M. Helfrich, L.K. Mangeney-Slavin, C.D. Keating, Dynamic microcompartmentation in synthetic cells, PNAS 102 (2005) 5920–5925.
[9] R. Hancock, Internal organisation of the nucleus: assembly of compartments by macromolecular crowding and the nuclear matrix model, Biol. Cell 96 (2004) 595–601.
[10] K. Rippe, Dynamic organization of the cell nucleus, Curr. Opin. Genet. Dev. 17 (2007) 373–380.
[11] K. Richter, M. Nessling, P. Lichter, Macromolecular crowding and its potential impact on nuclear function, Biochim. Biophys. Acta 1783 (2008) 2100–2107.
[12] F. Iborra, Can viscoelastic phase separation, macromolecular crowding and colloidal physics explain nuclear organisation? Theor. Biol. Med. Model. 4 (2007) 15.
[13] J. Shively, Complex Intracellular Structures in Prokaryotes, Springer, Berlin, 2006.
[14] N. Asherie, Protein crystallization and phase diagrams, Methods 34 (2004) 266–272.
[15] J.D. Gunton, A. Shiryayev, D.L. Pagan, Protein condensation: kinetic pathways to crystallization and disease, Cambridge University Press, 2007.
[16] A.P. Minton, Macromolecular crowding, Curr. Biol. 16 (2006) R269–R271.
[17] R.P. Sear, Specific protein–protein binding in many-component mixtures of proteins, Phys. Biol. 1 (2004) 53.
[18] J. Zhang, S. Maslov, E.I. Shakhnovich, Constraints imposed by non-functional protein–protein interactions on gene expression and proteome size, Mol. Syst. Biol. 4 (2008) 210.
[19] M. Hlevnjak, G. Zitkovic, B. Zagrovic, Hydrophilicity matching a prerequisite for the formation of protein–protein complexes, Preprint.
[20] P. Prinsen, T. Odijk, Optimized Baxter model of protein solutions: electrostatics versus adhesion, J. Chem. Phys. 121 (2004) 6525–6537.
[21] F.N. Braun, J. Bergenholtz, Glassy arrest in colloidal fluids with size polydispersity, J. Phys. Chem., B 111 (2007) 11626.
[22] J. Hansen, I. McDonald, Theory of Simple Liquids, Academic Press, London, 2006.
[23] A. Stradner, et al., Equilibrium cluster formation in concentrated protein solutions and colloids, Nature 432 (2004) 492.

[24] F.N. Braun, S. Paulsen, R.P. Sear, P.B. Warren, Miscibility gap in the microbial fitness landscape, Phys. Rev. Lett. 94 (2005) 178105.
[25] G.G. Tartaglia, S. Pechmann, C.M. Dobson, M. Vendruscolo, Life on the edge: a link between gene expression levels and aggregation rates of human proteins, Trends Biochem. Sci. 32 (2007) 204.
[26] J.M. Wood, Osmosensing by bacteria, Sci. STDKE 357 (2006) e43.
[27] G. Bogaart, N. Hermans, V. Krasnikov, B. Poolman, Protein mobility and diffusive barriers in E. coli: consequences of osmotic stress, Mol. Microbiol. 64 (2007) 858–871.
[28] F.N. Braun, Salting-in the microbial cytoplasm, FEBS Lett. 580 (2006) 720.
[29] J.R. Blackwell, R. Horgan, A novel strategy for production of a highly expressed recombinant protein in an active form, FEBS Lett. 295 (1991) 10–12.
[30] V. Dakos, et al., Slowing down as an early warning signal for abrupt climate change, PNAS 105 (2008) 14308–14312.
[31] J.E. Ferrell, Tripping the switch fantastic: how a protein kinase cascade can convert graded inputs into switch-like outputs, Trends Biochem. Sci. 21 (1996) 460.
[32] M. Samoilov, S. Plyasunov, A.P. Arkin, Stochastic amplification and signaling in enzymatic futile cycles through noise-induced bistability with oscillations, PNAS 102 (2005) 2310–2315.
[33] C.C. Guet, M.B. Elowitz, W. Hsing, S. Leibler, Combinatorial synthesis of genetic networks, Science 296 (2002) 1466.
[34] Y. Ishihama, et al., Protein abundance profiling of the E. coli cytosol, BMC Genomics 9 (2008) 102.
[35] D.S. Goodsell, Inside a living cell, Trends Biochem. Sci. 16 (1991) 203–206.
[36] R.P. Sear, The cytoplasm of living cells: a functional mixture of thousands of components, J. Phys., Condens. Matter 17 (2005) S3587–S3595.
[37] R.P. Sear, J. Cuesta, Instabilities in complex mixtures with a large number of components, Phys. Rev. Lett. 91 (2003) 245701.
[38] E. Pennisi, Evolutionary biology. The birth of the nucleus, Science 305 (2004) 766–786.
[39] W. Martin, E. Koonin, Introns and the origin of nucleus–cytosol compartmentalization, Nature 440 (2006) 41–45.
[40] P.B. Warren, Fluid–fluid phase separation in hard spheres with a bimodal size distribution, Europhys. Lett. 46 (1999) 295–300.